

Horizons and Correlation Functions in 2D Schwarzschild-de Sitter Spacetime

Paul Anderson^(a) and Jennie Traschen^(b)

^(a) Department of Physics, Wake Forest University, Winston-Salem, NC 27109, USA

^(b) Department of Physics, University of Massachusetts, Amherst, MA 01003, USA

Email: anderson@wfu.edu, traschen@umass.edu

Abstract

The two-point correlation function, and the two point function for the field velocities, are computed for a massless minimally coupled scalar field in 2D Schwarzschild-de Sitter spacetime when the field is in the Unruh state. It is found that the field correlations grow linearly in terms of a particular time coordinate that is good throughout the spacetime, and that the rate of growth is equal to the sum of the black hole plus cosmological surface gravities. This time dependence of the two-point function results from additive contributions from each horizon component of the past Cauchy surface that is used to define the Unruh state. The velocity two-point function is similar to that in Minkowski space when the two points are not separated by either the black hole or cosmological horizon. It vanishes when one point is on the black hole horizon and one point is on the cosmological horizon. If the two points are separated radially but not temporally and one point is fixed on a horizon, then a peak always occurs. In addition, peaks sometimes develop when the two points are separated by a horizon.

I. INTRODUCTION

Studies of quantum fields in black hole and cosmological spacetimes have found important and fascinating phenomena, including Hawking radiation from black hole and cosmological horizons [1][2] and the prediction that quantum fluctuations during inflation lead to density fluctuations in the early universe [3] [4]. The dynamics of quantum fluctuations in inflationary universe models are controlled on large scales by the cosmological horizon, and the results of these calculations agree exceedingly well with precision observations of anisotropies in the Cosmic Microwave Background Radiation (CMBR). In fact observations are so good that deviations from scale-invariance have been detected, and have motivated much exploration of inflation models to identify causes for the deviations. Recently, LIGO detections of gravitational waves have introduced another potential source of information about the early universe, and have lead to renewed interest in the possibility of primordial black holes [5] [6] [7] [8]. See [9] for an analysis based on quantum gravity considerations, and [10] for an analysis based on Λ CDM phenomenology, plus compilations of references relevant to these different perspectives. If black holes existed in the early universe it is possible that the effects could be observed in the CMBR. In this case the spectrum of quantum fluctuations would be the result of the dynamics of the cosmological and black hole horizons.

The key ingredient in calculations of the power spectrum of fluctuations in inflation is the two-point function for a quantum scalar field. In early calculations the background spacetime was taken to be de Sitter during the inflationary period, matched to a standard FRW cosmology after inflation. Subsequent research proceeded to more realistic inflating spacetime backgrounds, see *e.g.* [11] for a general introduction and [12] for a more recent review and analysis of various contributions to deviations from scale invariance in the power spectrum.

Similarly, to incorporate black holes into inflationary models the simplest place to begin is Schwarzschild-de Sitter spacetime (SdS) which is an exact black hole solution to the Einstein equations with a positive cosmological constant. In references [13] [14][15] the perturbation to the Green's function in four-dimensional SdS is computed in the limit of small black holes, and the state is approximated as the Bunch-Davies state. Due to the technical challenges in $4D$, the results are extracted by a combination of analytic approximations and numerical work.

In this paper we take a complementary approach and consider a massless minimally coupled scalar field in SdS in two dimensions ($2D$). This simplification makes it possible to find exact analytic solutions to the mode equation for any size black hole. We focus on the symmetric two-point correlation function, or Hadamard Green's function, and on the velocity correlation function that can be derived from it. In spite of the substantial simplifications that occur in $2D$, nontrivial quantum effects still occur. It turns out that there is no useful analog of the power spectrum computation in $2D$, so we defer that to a later $4D$ investigation.

Our calculations are done for a generalization of the Unruh vacuum in Schwarzschild spacetime [16] to SdS [17], in which particle states are defined with respect to an affine parameter on the past black hole and cosmological horizons, also referred to as Kruskal coordinates. It has been shown [17] that this state gives the same behavior for the stress-energy tensor as is found at late times in the case of an SdS black hole that forms from the collapse of a massive shell in $2D$. Since we are ultimately interested in black holes that form from collapse in the early universe, the Unruh state is the natural one for us to consider. We compute the two-point correlation function $G^{(1)}$ in SdS when the massless scalar field is in the Unruh state and then focus on correlations between points on slices of constant time T . Here T is a Killing timelike coordinate that is well-behaved throughout the spacetime. It is relevant for a black hole in slow roll inflation[18] [19], as will be discussed below. We find that $G^{(1)}$ increases linearly in T with the rate determined by the sum of the surface gravities of the black hole and cosmological horizons,

$$2\pi G^{(1)}(T, r_1, T, r_2) = (\kappa_b + \kappa_c)T + (r_1, r_2 \text{ dependent term}) \quad (1.1)$$

To understand this result, the two-point functions in $2D$ Minkowski, Schwarzschild, and deSitter spacetimes are computed. $G^{(1)}$ is also found for the more complicated examples of null shell-collapse to a black hole, and a Bose-Einstein condensate (BEC) analog black hole. We argue that the form of the time dependence in (1.1) arises from the relation between the geodesic and the Killing coordinates on a horizon J , and that there is a contribution of $\kappa_J T$ from each horizon that is a component of the past Cauchy surface.

We also compute the two-point correlation function for the field “velocities” $\partial_T \phi$. On constant T slices there are peaks due to the presence of the horizons. A similar peak

occurs for the density-density correlation function of a BEC analog black hole [20–22]. The spacetime that corresponds to the analog model is a 2D black hole, which comes from an acoustic horizon in the BEC. Laboratory experiments [23, 24] have confirmed the existence of this peak. A theoretical model has also been constructed for an analog cosmological horizon system [25] which focused on analog Hawking radiation.

For SdS we find that the velocity two-point function looks most like that for Minkowski spacetime when the two points are not separated by a horizon. It vanishes when one point is on the black hole horizon and the other is on the cosmological horizon. If one point is fixed to the cosmological horizon and the other is allowed to vary inside the black hole, then there is always a peak. Similarly there is always a peak when one point is fixed to the black hole horizon and the other is allowed to vary outside the cosmological horizon. When neither point is on a horizon peaks also occur when the points are separated by one or both horizons. Hence the horizons act as a watershed for a surprisingly rich behavior.

This paper is organized as follows. The coordinate systems that we use for SdS are summarized in Section II. In Section III, the Unruh vacuum for SdS is defined and the two-point function $G^{(1)}$ for ϕ is computed. In Section IV, $G^{(1)}$ is computed in the Unruh vacuum for several other spacetimes and its time dependence is analyzed. The two-point function g for the velocity $\partial_T \phi$ is computed in Section V. Plots of $G^{(1)}$ and g are contained in these two sections. In Section VI the connection between the Unruh SdS vacuum and the Bunch-Davies vacuum in the cosmological far field region is studied. In Section VI B, the time dependence of G in 4D de Sitter is shown. Concluding remarks are contained in Sec. VII. In Appendix A, an alternative way to calculate the two-point function that is useful in 4D calculations is described. The method is applied to 2D SdS and it is shown to miss the term that grows linearly in time. Appendix B contains an alternative computation of the velocity correlation function.

II. SOME USEFUL COORDINATE SYSTEMS FOR SDS

There are several sets of coordinates that we find useful for SdS. Here we review those coordinates and the relations between them.

First in the static region between the black hole and cosmological horizons one can define

the usual static coordinates for which the metric is

$$ds^2 = -f dt^2 + \frac{1}{f} dr^2 = f(-dt^2 + dr_*^2) \quad (2.1)$$

with

$$f(r) = 1 - \frac{2M}{r} - H^2 r^2 = -\frac{H^2}{r}(r - r_c)(r - r_b)(r + r_c + r_b) \quad (2.2)$$

Here $r_c > r_b$ are the locations of the cosmological and black hole horizons respectively, and $\frac{1}{3}\Lambda = \ell)c^{-2} = H^2$. The two parameterizations are related by

$$M = \frac{r_b r_c (r_b + r_c)}{2(r_b^2 + r_c^2 + r_b r_c)}, \quad H^2 = \frac{1}{r_b^2 + r_c^2 + r_b r_c} \quad (2.3)$$

For SdS Λ is positive and there is a maximal area for the black hole which occurs when $r_c = r_b = 1/(\sqrt{3}H)$, corresponding to a maximal mass of $M_{max} = 1/(3\sqrt{3}H)$ and, as shown below, a surface gravity of zero.

The tortoise coordinate r_* is defined by

$$r_*(r) = \int \frac{dr}{f}. \quad (2.4)$$

An explicit expression is given for it in (2.17). The ingoing and outgoing radial null coordinates are

$$u = t - r_*, \quad v = t + r_*. \quad (2.5)$$

The wave equation for the massless minimally coupled scalar field can be written conveniently as

$$(\partial_t^2 - \partial_{r_*}^2) \phi = \partial_u \partial_v \phi = 0. \quad (2.6)$$

Hence the solutions are freely propagating waves which can be written as the sum of an arbitrary function of u and an arbitrary function of v .

Though the static coordinates t and r_* are useful for finding solutions to the wave equation, they are singular on the horizons, so it is useful to introduce Kruskal coordinates which are well-behaved on the horizons. Because there are two sets of past and future horizons in SdS one can define one set of Kruskal coordinates (U_b, V_b) with respect to the black hole horizons and a second set (U_c, V_c) with respect to the cosmological horizons. The coordinate

U_b is a geodesic coordinate on the past black hole horizon \mathcal{H}_b^- , and is equal to zero on the future one, \mathcal{H}_b^+ , while V_b is zero on \mathcal{H}_b^- and a geodesic coordinate on \mathcal{H}_b^+ . Similarly V_c is a geodesic coordinate on the past cosmological horizon, \mathcal{H}_c^- , and is zero on the future one \mathcal{H}_c^+ , while U_c is a geodesic coordinate on \mathcal{H}_c^+ and zero on \mathcal{H}_c^- .

To find the relationships between the various Kruskal coordinates and the static coordinates u and v , note that on the past black hole horizon u is regular while v diverges, and *vice versa* on the future black hole horizon. On the past cosmological horizon u diverges while v is regular with the opposite occurring on the future cosmological horizon.

For this paper we are interested in the region outside the past black hole horizon. Throughout that region

$$V_b = \frac{1}{\kappa_b} e^{\kappa_b v} , \quad (2.7)$$

while

$$U_b = \frac{1}{\kappa_b} e^{-\kappa_b u} , \quad r < r_b , \quad (2.8a)$$

$$= -\frac{1}{\kappa_b} e^{-\kappa_b u} , \quad r > r_b , \quad (2.8b)$$

with κ_b the surface gravity of the black hole horizon. We are also interested in the region outside the past cosmological horizon. Throughout that region

$$U_c = \frac{1}{\kappa_c} e^{\kappa_c u} , \quad (2.9)$$

while

$$V_c = -\frac{1}{\kappa_c} e^{-\kappa_c v} , \quad r < r_c , \quad (2.10a)$$

$$= \frac{1}{\kappa_c} e^{-\kappa_c v} , \quad r > r_c , \quad (2.10b)$$

with κ_c the surface gravity of the cosmological horizon. Solving (2.7) for v , solving (2.9) for u and using these in (2.10) and (2.8) respectively, one finds in the static patch, $r_b < r < r_c$ the following relationships between the two sets of coordinates

$$\kappa_c V_c = -(\kappa_b V_b)^{-\kappa_c/\kappa_b} , \quad \kappa_b U_b = -(\kappa_c U_c)^{-\kappa_b/\kappa_c} . \quad (2.11)$$

A set of coordinates that are good across the future black hole and cosmological horizons were found in [18][19]. Let

$$T = t + h(r) , \quad \text{where} \quad \frac{dh}{dr} = \frac{j}{f} , \quad j(r) = -\gamma r + \frac{\beta}{r^2} , \quad (2.12)$$

and

$$\gamma = \frac{r_c^2 + r_b^2}{r_c^3 - r_b^3} , \quad \beta = \frac{r_c^2 r_b^2 (r_b + r_c)}{r_c^3 - r_b^3} . \quad (2.13)$$

Then the 2D SdS metric becomes¹

$$ds^2 = -f(r)dT^2 + 2j(r)drdT + \frac{1 - j^2}{f}dr^2 . \quad (2.14)$$

The constants γ and β have been chosen such that $j(r_b) = 1$ and $j(r_c) = -1$, which ensures that T interpolates between the ingoing null coordinate v at the future black hole horizon and the outgoing null coordinate u at the future cosmological horizon. These are ingoing and outgoing Eddington-Finklestein coordinates respectively. Physically, the T coordinate is a time coordinate for a slowly rolling inflaton field in 4D. The metric (2.14) is well behaved in the static and cosmological regions and has the Eddington-Finklestein form on both the future black hole and future cosmological horizons. The coordinate T stays timelike and r stays spacelike beyond the cosmological horizon.

The integrations for r_* and T each contain an arbitrary constant which we choose such that

$$T = u \text{ on } \mathcal{H}_c^+ , \quad \text{and} \quad T = v \text{ on } \mathcal{H}_b^+ . \quad (2.15)$$

We find

$$\begin{aligned} T &= t + h(r) \\ &= t + \frac{1}{2\kappa_b} \log \frac{|r - r_b|}{r_c - r_b} + \frac{1}{2\kappa_c} \log \frac{|r - r_c|}{r_c - r_b} + \frac{1}{2} \left(\frac{r_c}{r_b \kappa_b} - \frac{1}{\kappa_N} \right) \log \frac{r + r_c + r_b}{r_c + 2r_b} \\ &\quad - \frac{r_b r_c}{2(r_c - r_b)} \log \frac{r^2}{r_c r_b} + \frac{r_c}{4r_b \kappa_b} \log \frac{r_c + 2r_b}{2r_c + r_b} , \end{aligned} \quad (2.16)$$

¹ The 4D SdS metric in these coordinates has an additional $r^2 d\Omega^2$ term.

and

$$\begin{aligned} r_*(r) &= \frac{1}{2\kappa_b} \log \frac{|r - r_b|}{r_c - r_b} - \frac{1}{2\kappa_c} \log \frac{|r - r_c|}{r_c - r_b} + \frac{1}{2\kappa_N} \log \frac{|r + r_c + r_b|}{r_c + 2r_b} \\ &\quad - \frac{r_c}{4r_b\kappa_b} \log \frac{2r_c + r_b}{r_c + 2r_b} - \frac{r_b r_c}{2(r_c - r_b)} \log \frac{r_b}{r_c}, \end{aligned} \quad (2.17)$$

where for a horizon at $r = r_h$ we set $2\kappa_h = |f'(r_h)|$ so that all of the surface gravities denote positive quantities. Note that r_N and κ_N refers to the negative root of $f(r)$ at $r_N = -(r_b + r_c)$. While this root exists mathematically, the spacetime ends at $r = 0$ where there is a curvature singularity. For future use, the surface gravities are given by

$$\begin{aligned} \kappa_b &= \frac{H^2}{2r_b} (r_c - r_b)(r_c + 2r_b), \\ \kappa_c &= \frac{H^2}{2r_c} (r_c - r_b)(2r_c + r_b), \\ \kappa_N &= \frac{H^2}{2(r_c + r_b)} (2r_c + r_b)(r_c + 2r_b). \end{aligned} \quad (2.18)$$

While there are several quantities of geometrical interest, including H, M, r_b, r_c, κ_b and κ_c , it is important to recall that SdS is only a two-parameter family of solutions. We will generally take the two independent parameters to be H and r_b .

To relate the Kruskal coordinates to T and r , note that $u = T - (h(r) + r_*)$ and $v = T - h(r) + r_*$. Substitution gives

$$V_c = \frac{1}{\kappa_c} e^{-\kappa_c T} \tilde{V}_c, \quad \text{and} \quad U_b = \frac{1}{\kappa_b} e^{-\kappa_b T} \tilde{U}_b, \quad (2.19)$$

where \tilde{U}_b and \tilde{V}_c only depend on r and are given by

$$\begin{aligned} \tilde{V}_c &= e^{\kappa_c(h-r_*)} = \frac{r - r_c}{r_c - r_b} \left(\frac{r + r_c + r_b}{r_c + 2r_b} \right)^{r_b/2r_c} \left(\frac{r_b}{r} \right)^{H^2 r_b (2r_c + r_b)/2}, \\ \tilde{U}_b &= -e^{\kappa_b(h+r_*)} = -\frac{(r - r_b)}{r_c - r_b} \left(\frac{r + r_b + r_c}{2r_c + r_b} \right)^{r_c/2r_b} \left(\frac{r_c}{r} \right)^{H^2 r_c (r_c + 2r_b)/2}. \end{aligned} \quad (2.20)$$

These expressions can be used in any region, that is, there is no longer a set of different cases. When working through the algebra, one finds that the different signs in the relations for the transformations between U_b, V_c and u, v given in (2.8) and (2.10) are compensated for by the different cases encoded in the absolute value signs in h and r_* .

III. TWO-POINT FUNCTION FOR SDS IN THE UNRUH STATE

The generalized SdS Unruh vacuum [17] defines particle states on the past Cauchy surface $\mathcal{H}_b^- \cup \mathcal{H}_c^-$ with respect to modes that are well behaved on the horizons. Black hole and cosmological particle production in the Unruh vacuum was computed in [26]. Using the Kruskal coordinates, the boundary conditions on the past modes are

$$p_\omega^b = \frac{1}{\sqrt{4\pi\omega}} e^{-i\omega U_b} \quad \text{on } \mathcal{H}_b^- , \quad (3.1a)$$

$$= 0 \quad \text{on } \mathcal{H}_c^- \quad (3.1b)$$

$$p_\omega^c = \frac{1}{\sqrt{4\pi\omega}} e^{-i\omega V_c} \quad \text{on } \mathcal{H}_c^- , \quad (3.1c)$$

$$= 0 \quad \text{on } \mathcal{H}_b^- . \quad (3.1d)$$

The enormous simplification in $2D$ is that these functions are solutions to the wave equation throughout the spacetime.

The expansion for the field in terms of Kruskal modes is

$$\phi = \int_0^\infty d\omega \left[a_\omega^b p_\omega^b + a_\omega^c p_\omega^c + a_\omega^{b\dagger} p_\omega^{b*} + a_\omega^{c\dagger} p_\omega^{c*} \right] , \quad (3.2)$$

where the a_ω^b and a_ω^c annihilate the Unruh vacuum

$$a_\omega^b |0\rangle = a_\omega^c |0\rangle = 0 . \quad (3.3)$$

The creation and annihilation operators are normalized as

$$[a_\omega^h, a_{\omega'}^{h'\dagger}] = \delta(\omega - \omega') \delta^{h,h'} \quad , \quad h, h' = b, c . \quad (3.4)$$

The symmetric Green's function is

$$G^{(1)}(x, x') = \langle 0 | \phi(x) \phi(x') + \phi(x') \phi(x) | 0 \rangle . \quad (3.5)$$

Substituting (3.2) into (3.5) and using (3.3) and (3.4) gives

$$\begin{aligned}
G(x, x') &= \int_0^\infty d\omega [p_\omega^b(x)p_\omega^{b*}(x') + p_\omega^b(x')p_\omega^{b*}(x) + p_\omega^c(x)p_\omega^{c*}(x') + p_\omega^c(x')p_\omega^{c*}(x)] \\
&= \frac{1}{2\pi} \int_{\omega_0}^\infty \frac{d\omega}{\omega} \left\{ \cos[\omega(U_b - U'_b)] + \cos[\omega(V_c - V'_c)] \right\} \\
&= -\frac{1}{2\pi} \left\{ ci[\omega_0|U_b - U'_b|] + ci[\omega_0|V_c - V'_c|] \right\}. \tag{3.6}
\end{aligned}$$

with ci the cosine integral function and ω_0 an arbitrary infrared cutoff. We have dropped the superscript (1) on G since we will only be considering the symmetric Greens function.

If G is used to compute, for example, the stress-energy tensor then one takes derivatives of G with respect to the coordinates. After doing so there is no infrared divergence and ω_0 can be set equal to zero. Here we restrict our attention to point separations and values of ω_0 such that $|\omega_0\Delta U_b| \ll 1$ and $|\omega_0\Delta V_c| \ll 1$. This can clearly be done for any fixed separation of the points by taking ω_0 to be small enough. However, it is important to remember that however small the value of ω_0 may be, once its value is fixed, there will always be point separations that are large enough to violate these conditions. When these conditions are satisfied, only the first two terms in the expansions for the cosine integrals are significant and one can take

$$2\pi G(x, x') = -2\gamma_E - \log \omega_0^2 |\Delta U_b \Delta V_c|, \tag{3.7}$$

where γ_E is Euler's constant.

A. Correlations on equal time slices

Next we analyze the behavior of the correlation function when the two points have the same time coordinate T , since this is a good time coordinate in the static and cosmological regions and on the horizons. The case when one point is on each horizon is particularly simple, and provides guidance for the general case.

1. Horizon to Horizon Correlations

Let x_1 be on \mathcal{H}_b^+ and x_2 on \mathcal{H}_c^+ . Then $U_{b1} = 0$ and $V_{c2} = 0$. Using (2.8), (2.10), (2.11), and (2.15) gives

$$\Delta U_b = -\frac{1}{\kappa_b}(\kappa_c U_{c2})^{-\kappa_b/\kappa_c} = -\frac{1}{\kappa_b}e^{-\kappa_b T}, \quad (3.8a)$$

$$\Delta V_c = \frac{1}{\kappa_c}(\kappa_b V_{b1})^{-\kappa_c/\kappa_b} = \frac{1}{\kappa_c}e^{-\kappa_c T}. \quad (3.8b)$$

Substituting into (3.7) then gives

$$2\pi G(x_1, x_2) = (\kappa_b + \kappa_c)T - \log\left(\frac{\omega_0^2}{\kappa_b \kappa_c}\right) - 2\gamma_E. \quad (3.9)$$

Correlations between the horizons grow linearly in T with the growth rate set by the sum of the surface gravities.

2. General case

Next we analyze G for two points that have the same T coordinate but otherwise can be anywhere. Substituting U_b and V_c given in (2.19) and (2.20) into (3.7) yields

$$2\pi G(x_1, x_2) = T(\kappa_b + \kappa_c) - \log\left(\frac{\omega_0^2}{\kappa_b \kappa_c} |\Delta \tilde{U}_b \Delta \tilde{V}_c|\right) - 2\gamma_E. \quad (3.10)$$

Hence we learn that quite generally for points at the same time T , G increases in time like $T(\kappa_b + \kappa_c)$. This is one of our main results.

We have not found this time dependence mentioned in the literature for either static black holes or black holes that form from collapse in $2D$. It was also not previously known for Bose-Einstein condensate analog black holes. In the Appendix we show that certain techniques that work in $4D$ miss the time contribution in $2D$ because of the infrared divergence in the $2D$ two-point function. This time dependence does not happen for quantities such as the stress-energy tensor for the scalar field in the black hole case, or the density-density correlation function in the BEC analog black hole case, since they involve derivatives of the two-point function that remove the infrared divergence.

The spatially dependent part of $G(x_1, x_2)$ is

$$2\pi\bar{G}(r_1, r_2) \equiv -\log(|\Delta\tilde{U}_b\Delta\tilde{V}_c|) \quad (3.11)$$

where \tilde{U}_b, \tilde{V}_c are given in (2.20). The correlation function (3.11) is not translation invariant, so its value depends on the location of each point. One way of plotting this is shown in Fig. 1. Note that as usual the Green's function diverges on the coincidence line $r_1 = r_2$,

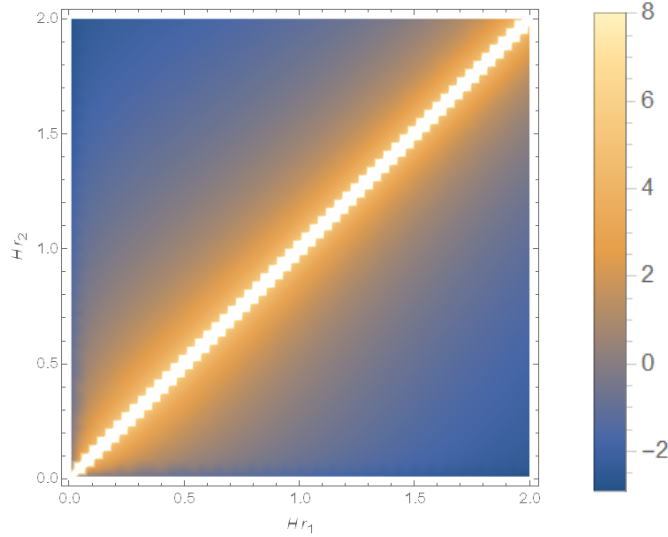


FIG. 1: Density plot of $\bar{G}(r_1, r_2)$ for $Hr_b = 0.2$. The horizontal axis is Hr_1 and the vertical axis is Hr_2 .

and then decreases monotonically away from this line in both directions. Thus the most interesting feature of $G(x_1, x_2)$ is its time dependence. As shown below, the two-point function for the time derivative of the field, $\partial_T\phi$, has more structure.

IV. κT DEPENDENCE IN OTHER 2D SPACETIMES

Having found the simple linear time dependence of G , and that the sum of the surface gravities determines the rate of change of correlations, it is useful to compare these results to the corresponding correlation functions in Minkowski, Schwarzschild, and de Sitter spacetimes. We also compute the correlation function in the spacetime of a null shell that collapses to form a Schwarzschild black hole, and in the BEC analog black hole metric. In each case particle states are defined with respect to geodesic coordinates on a past Cauchy surface. If part of the Cauchy surface is a horizon, then this will be a Kruskal type coor-

dinate. With this rule, we will show that each past horizon contributes a time dependence of $\kappa_J T$ to G , where T is a good ‘lab time’ coordinate. For spacetimes with one or more past horizons, this behavior is expected in general to be based on basic properties of Killing horizons. For spacetimes with no past horizon but one or more future horizons the situation is more complicated as is shown below for the collapsing null shell spacetime. We now turn to these examples, which ‘deconstruct’ the SdS case.

A. Minkowski Spacetime

In $1 + 1$ dimensions we take

$$ds^2 = -dt^2 + dr^2 = -dudv, \quad (4.1)$$

where $u = t - r$, $v = t + r$ as before, and all the coordinates range between plus and minus infinity. An early time Cauchy surface can be taken to be the union of the two branches of past null infinity, and the modes are

$$p_\omega^{in} = \frac{1}{\sqrt{4\pi\omega}} e^{-i\omega(t-r)}, \quad p_\omega^{out} = \frac{1}{\sqrt{4\pi\omega}} e^{-i\omega(t+r)}. \quad (4.2)$$

The Green’s function is derived by the same steps as in (3.6) and (3.7) with p^b replaced by p^{in} and p^c replaced by p^{out} , which gives

$$2\pi G_M(x_1, x_2) = -\log|\omega_0^2 \Delta u \Delta v| \quad (4.3a)$$

$$= -\gamma_E - \log|\omega_0 \Delta r|^2 - 2\gamma_E, \quad t_1 = t_2 \quad (4.3b)$$

labelgflat At equal times the Green’s function is independent of t .

B. Schwarzschild Spacetime

Setting $H = 0$ in (2.14) gives the Schwarzschild metric in (T, r) coordinates,

$$ds^2 = -(1 - \frac{r_b}{r})dT^2 + 2\frac{r_b^2}{r^2}drdT + (1 + \frac{r_b}{r})dr^2, \quad (4.4)$$

which is good on the black hole horizon, where T becomes the ingoing null coordinate v . The surface gravity is $\kappa_b = 1/(2r_b)$. The past Cauchy surface is now the past black hole horizon plus past null infinity \mathcal{I}^- . The particle states on \mathcal{H}_b^- are defined by the modes $p_\omega^b(U_b)$ as in SdS, and states on \mathcal{I}^- are defined with respect to the ingoing modes in static coordinates $p_\omega^\infty(v)$. Then the calculation of G_S follows the same steps as in SdS that lead to (3.6), but with $p_\omega^\infty(v) = e^{-i\omega v}/\sqrt{4\pi\omega}$ replacing $p_\omega^c(V_c)$, which gives the Schwarzschild Greens function in the Unruh vacuum,

$$\begin{aligned} 2\pi G_{S,U}(x_1, x_2) &= -\log |\omega_0^2 \Delta U_b \Delta v| - 2\gamma_E \\ &= -\log \frac{\omega_0^2}{\kappa_b} |\Delta(e^{\kappa_b(-T+r_*+h)}) \Delta(T+r_*-h)| - 2\gamma_E . \end{aligned} \quad (4.5)$$

In the second line we have used $U_b = -e^{-\kappa_b u}/\kappa_b$, $u = T - h - r_*$, and $v = T - h + r_*$. This is distinct from the Hartle-Hawking vacuum, which is explicitly constructed to be thermal.

Setting $T_1 = T_2 = T$ we see that $G_{S,U}$ increases in time like $\kappa_b T$,

$$2\pi G_{S,U}(x_1, x_2) = \kappa_b T - 2\gamma_E - \log \left| \frac{\omega_0^2}{\kappa_b} (e^{\kappa_b(h+r_*)_2} - e^{\kappa_b(h+r_*)_1})(r_{*2} - h_2 - r_{*1} + h_1) \right| , \quad (4.6)$$

where the spatial dependence is explicitly given by

$$h(r) + r_* = r + r_b \left(2 \log \frac{|r - r_b|}{r_b} - \log \frac{r}{r_b} \right) , \quad r_* - h(r) = r + r_b \log \frac{r}{r_b} . \quad (4.7)$$

There is only one surface gravity factor in $G_{S,U}$ since there is only one past horizon.

Rather than using the (T, r) coordinates, G could be evaluated in the static Schwarzschild (t, r) coordinates. The difference would be logarithmic corrections which are subdominant at infinity, but relevant near the black hole horizon. $G(T, r)$ is well behaved when one point is on the horizon, whereas in the static coordinates $G(t, r)$ is not. For example, setting $r_1 = r_b$ and $r_2 = r \gg r_b$ in (4.6) gives

$$2\pi G_S(r_b, r) \simeq \kappa_b(T - r) - \frac{3}{2} \log(\omega_0 r) \quad (4.8)$$

C. de Sitter Spacetime

Setting $M = 0$ in (2.14) gives the 2D de Sitter metric in coordinates that are good on the cosmological horizon,

$$ds^2 = -(1 - H^2 r^2) dT^2 - 2H r dT dr + dr^2 . \quad (4.9)$$

These are related to the usual static coordinates with metric

$$ds^2 = -(1 - H^2 r^2) dt^2 + \frac{dr^2}{1 - H^2 r^2} , \quad (4.10)$$

by the relation

$$T = t + \frac{1}{2H} \log |1 - H^2 r^2| . \quad (4.11)$$

The tortoise coordinate

$$r_* = \frac{1}{2H} \log \left| \frac{1 + Hr}{1 - Hr} \right| , \quad (4.12)$$

can be used to put the metric (4.10) in the conformally flat form

$$ds^2 = (1 - H^2 r^2) (-dt^2 + dr_*^2) . \quad (4.13)$$

It is also useful to work with the usual spatially flat (in 4D) cosmological coordinates for which the metric in 2D is

$$ds^2 = -d\tau^2 + a^2 d\rho^2 = a^2 (-d\eta^2 + d\rho^2) , \quad (4.14)$$

with the scale factor

$$a = e^{H\tau} = \frac{-1}{H\eta} . \quad (4.15)$$

The coordinate transformation between the static and cosmological coordinates is

$$\tau = t + \frac{1}{2H} \log |1 - H^2 r^2| = T , \quad (4.16a)$$

$$\rho = \frac{r e^{-Ht}}{\sqrt{1 - H^2 r^2}} . \quad (4.16b)$$

Inverting these one finds

$$r = \rho e^{H\tau} = -\frac{\rho}{H\eta}, \quad (4.17a)$$

$$t = \tau - \frac{1}{2H} \log |1 - H^2 r^2|. \quad (4.17b)$$

In 2D de Sitter space there are cosmological horizons at $r = \pm H^{-1}$ which in terms of the cosmological coordinates translates to $\eta = \pm \rho$.

In de Sitter space an early time Cauchy surface can be taken to be the union of the two branches of the past cosmological horizon. Because the massless minimally coupled scalar field is conformally invariant in 2D and the spacetime is conformally flat, the general solution to the wave equation can be written as a function of $(\eta + \rho)$ and a function of $(\eta - \rho)$. The Bunch-Davies state is defined by the positive frequency modes

$$p_\omega^{in} = \frac{1}{\sqrt{4\pi\omega}} e^{-i\omega(\eta-\rho)}, \quad p_\omega^{out} = \frac{1}{\sqrt{4\pi\omega}} e^{-i\omega(\eta+\rho)}. \quad (4.18)$$

First we show that these modes are the same as Kruskal modes $e^{-i\omega U}$, $e^{-i\omega V}$. To see this first note that the Kruskal coordinates are defined in this case as

$$U = \frac{1}{H} e^{-Hu} \quad \text{and} \quad V = \frac{1}{H} e^{-Hv}, \quad (4.19)$$

with $u = t - r_*$, and $v = t + r_*$ as before. Note that the Cauchy surface is the union of two past cosmological horizons at $U = -\infty$ and $V = -\infty$, the future horizons being at $U = 0$ and $V = 0$. Using (4.11), (4.12), (4.15), and (4.17), one finds

$$U = |\eta - \rho|, \quad \text{and} \quad V = |\eta + \rho|. \quad (4.20)$$

Hence the Bunch-Davies state (4.18) is the same as the Unruh state. This choice of vacuum meshes well with the SdS case, but there are other choices of de Sitter states, for example the ‘Unruh-de Sitter’ state in [27].

The Green’s function then has the same form as (3.6) with p^b replaced by p^{out} and p^c

replaced by p^{in} . One finds for $T_1 = T_2 = T$ that

$$2\pi G_{dS}(x_1, x_2) = -\log |\omega_0^2 \Delta(\eta - \rho) \Delta(\eta + \rho)| - 2\gamma_E \quad (4.21a)$$

$$= -\log[e^{-2HT}(\omega_0 \Delta r)^2] - 2\gamma_E \quad (4.21b)$$

$$= 2HT - \log(\omega_0 \Delta r)^2 - 2\gamma_E . \quad (4.21c)$$

Noting that in de Sitter space, $H = \kappa_c$, the time dependence has the same form as was found in SdS with κ_b replaced by κ_c from the “other” past cosmological horizon.

D. Collapsing null shell spacetime

Perhaps the simplest way mathematically in which a black hole can form from collapse is by the collapse of a spherically symmetric null shell. In 2D it is possible to compute the two-point function for the massless minimally coupled scalar field analytically, and that is done here.

The shell starts at past null infinity \mathcal{I}^- and moves along the trajectory $v = v_0$ for some constant v_0 . Inside the shell the spacetime is flat. In 4D the mode functions must be regular at $r = 0$. Equivalent boundary conditions can be obtained by putting a static perfectly reflecting mirror at $r = 0$. Outside the shell the metric is that for Schwarzschild spacetime. In 4D, given that the radial coordinate r is related to the area of a two sphere, it is useful to have r be continuous across the shell and t discontinuous. Alternatively one can have v be continuous and u discontinuous. Letting the subscript F refer to coordinates in the interior flat region and imposing continuity of v gives $u = t - r_*$ and $u_F = t_F - r$ is [28, 29]

$$u = u_F - \frac{1}{\kappa} \log(\kappa(v_H - u_F)) , \quad (4.22)$$

with

$$v_H \equiv v_0 - 4M . \quad (4.23)$$

Inverting this gives [30]

$$u_F = v_H - \frac{1}{\kappa} W[e^{\kappa(v_H - u)}] , \quad (4.24)$$

with W the Lambert W function.

Inside the null shell the modes for the *in* vacuum state are

$$p_\omega^{\text{in}} = \frac{1}{\sqrt{4\pi\omega}}(e^{-i\omega v} - e^{-i\omega u_F}) . \quad (4.25)$$

Because the mode equation has the general solution $p = f(u_F) + g(v)$ in these coordinates this is the form of the solutions outside the null shell as well with $u_F(u)$ given by (4.24).

The two-point function (3.5) is

$$\begin{aligned} G(x, x') &= \int_0^\infty d\omega [p_\omega^{\text{in}}(x) p_\omega^{\text{in}*}(x') + p_\omega^{\text{in}}(x') p_\omega^{\text{in}*}(x)] \\ &= \frac{1}{2\pi} \int_{\omega_0}^\infty \frac{d\omega}{\omega} \{ \cos[\omega(v - v')] - \cos[\omega(v - u_F(u'))] - \cos[\omega(v' - u_F(u))] \\ &\quad + \cos[\omega(u_F(u) - u_F(u'))] \} \\ &= \frac{1}{2\pi} \{ -\text{ci}[\omega_0(v - v')] + \text{ci}[\omega_0(v - u_F(u'))] + \text{ci}[\omega_0(v' - u_F(u))] \\ &\quad - \text{ci}[\omega_0(u_F(u) - u_F(u'))] \} . \end{aligned} \quad (4.26)$$

Using $v = T - h(r) + r_*$ and $u = T - h(r) - r_*$, then at a late time T with r fixed,

$$u_F(u) \rightarrow v_H - \frac{1}{\kappa} e^{\kappa(v_H - u)} = v_H - \frac{1}{\kappa} e^{\kappa v_H} e^{-\kappa T} e^{\kappa(h(r) + r_*)}, \quad (4.27)$$

hence for both T and T' large

$$\begin{aligned} 2\pi G(x, x') &\rightarrow \frac{\kappa}{2}(T + T') - \text{ci}[\omega_0(v - v')] + \text{ci}[\omega_0(v - v_H)] + \text{ci}[\omega_0(v' - v_H)] \\ &\quad - \log |e^{\frac{\kappa}{2}[-(T-T') + 2(h(r) + r_*)]} - e^{\frac{\kappa}{2}[(T-T') + 2(h(r') + r'_*)]}| - \gamma_E - \log \left(\frac{\omega_0}{\kappa} \right) - \kappa v_H \end{aligned} \quad (4.28)$$

Setting $T' = T$, letting T get arbitrarily large while keeping the radial points fixed and choosing ω_0 small enough that $|\omega_0(v - v')| \ll 1$, one finds that

$$\begin{aligned} 2\pi G(x, x') &\rightarrow \kappa T - \log[\omega_0(v - v')] - \log \left(\frac{\omega_0}{\kappa} \right) \\ &\quad - \log |e^{\kappa(h(r) + r_*)} - e^{\kappa[(h(r') + r'_*)]}| - 2\gamma_E - \kappa v_H , \end{aligned} \quad (4.29)$$

where the behavior $\text{ci}(z) \rightarrow 0$ as $z \rightarrow \infty$ has been used. This is the same growth in time κT as that for static Schwarzschild spacetime when the field is in the Unruh state. Note that the growth only occurs in the late time limit. For early times $u_F \approx u$ and there is no linear

growth in T .

E. BEC analog black hole spacetime

In [20–22] a simple model of a Bose-Einstein condensate analog black hole was investigated. It was assumed that the BEC is effectively confined to one dimension with a steady flow and a sound speed $c(x)$ that varies with position along the flow. In some experiments [23, 24] and subsequent models [31, 32] the flow speed v_0 also varies with position. For a flow in the $-\hat{x}$ direction an analog black hole exists if there is a subsonic region where $v_0 < c$, and then to the left of this there is a supersonic region where $v_0 > c$. The sonic horizon occurs where $v_0 = c$. Theoretical models show that in the hydrodynamic or long wavelength approximation, the phonons satisfy a wave equation that has the same form as the wave equation for a massless minimally coupled scalar field in a certain spacetime. After dimensional reduction to 1+1 dimensions, the resulting mode equation is a 2D wave equation for a scalar field with an effective potential that depends on the sound speed and flow velocity profiles. So long as the sound speed and flow velocity approach constant values in the limits $x \rightarrow \pm\infty$, the spacetime associated with this wave equation has the same type of structure as Schwarzschild spacetime with the exception that there are no singularities inside the horizons.

In the original calculation of the BEC density-density correlation function [20] the effective potential in the mode equation for the phonons was ignored. This resulted in a mode equation that is the same as that for a massless minimally coupled scalar field in the analog spacetime. This is the approximation that we shall use here. The metric for the analog spacetime is

$$ds^2 = \frac{c(x)^2 - v_0(x)^2}{c(x)} (-dt^2 + dx_*^2) , \quad (4.30)$$

the tortoise coordinate is

$$x_* = \int^x dy \frac{c(y)}{c(y)^2 - v_0(y)^2} , \quad (4.31)$$

and the surface gravity of the analog black hole is

$$\kappa_b = \left. \left(\frac{dc}{dx} - \frac{dv_0}{dx} \right) \right|_{\text{hor}} . \quad (4.32)$$

One can then define the null coordinates $u = t - x_*$ and $v = t + x_*$.

For the BEC analog black hole experiments described in [23, 24], the density was measured throughout the condensate at a particular laboratory time T and used to compute the density-density correlation function. The laboratory time is given by the expression

$$T = t + \int^x dy \frac{v_0(y)}{c(y)^2 - v_0(y)^2} . \quad (4.33)$$

Using (4.33) and (4.31) in (4.30) one finds

$$ds^2 = -\frac{(c^2 - v_0^2)}{c} dT^2 + 2\frac{v_0}{c} dT dx + \frac{1}{c} dx^2 , \quad (4.34)$$

which is of the same form as (2.14) with $f = c^{-1}(c^2 - v_0^2)$, $j = \frac{v_0}{c}$, and $h = \int^x dy \frac{v_0(y)}{c(y)^2 - v_0(y)^2}$.

One finds that the null coordinates are

$$\begin{aligned} u &= T - \int^x \frac{dy}{c(y) - v_0(y)} , \\ v &= T + \int^x \frac{dy}{c(y) + v_0(y)} . \end{aligned} \quad (4.35)$$

As for Schwarzschild spacetime, in this BEC analog black hole spacetime the Cauchy surface can be taken to be a union of past null infinity and the past horizon, with particle states on \mathcal{H}_b^- defined by the modes $p_\omega^b(U_b)$, with U_b given by (2.8), and the particle states on \mathcal{I}^- are defined with respect to the ingoing modes in static coordinates $p_\omega^\infty(v)$. Hence the two-point function is

$$2\pi G_{\text{BEC},U}(T_1, x_1; T_2, x_2) = -2\gamma_E - \log |\omega_0^2 \Delta U_b \Delta v| . \quad (4.36)$$

This has the same form, (4.5), as it does for Schwarzschild spacetime. Setting $T_1 = T_2 = T$ one finds

$$\begin{aligned} 2\pi G_{\text{BEC},U}(T, x_1; T, x_2) &= -2\gamma_E + \kappa_b T - \log \left(\frac{\omega_0}{\kappa_b} \right) - \log \left| \omega_0 \int_{x_1}^{x_2} \frac{dx}{c(x) + v_0(x)} \right| \\ &\quad - \log \left| \exp \left(\kappa_b \int^{x_2} \frac{dy}{c(y) - v_0(y)} \right) \pm \exp \left(\kappa_b \int^{x_1} \frac{dy}{c(y) - v_0(y)} \right) \right| , \end{aligned} \quad (4.37)$$

where the plus sign occurs if one point is inside and the other point is outside the future horizon and the minus sign occurs if both points are on the same side of the horizon. As in the other 2D black hole cases there is a linear growth in T .

F. Generalizing: Killing horizons and time dependence

In the preceding examples the horizons are Killing horizons, except for the collapsing null shell spacetime which asymptotes to Schwarzschild spacetime. A key aspect in these calculations is that the affine parameter λ for the null geodesic generators of a Killing horizon is related on the horizon to the Killing parameter s by

$$\lambda \sim e^{\pm \kappa s}, \quad (4.38)$$

(see *e.g.* [33][34]) where the plus and minus options allow for our convention that κ is the magnitude of the surface gravity. In the examples worked out here, λ is one of the U or V coordinates. Extending the relation (4.38) off the horizon yields $s = T + R$ where T is a good timelike coordinate and R is a convenient spacelike coordinate. Specifically, in SdS the time coordinate T in (2.14) was arrived at as a well-behaved slow-roll coordinate for an inflaton in SdS, and is also a Killing parameter. In Minkowski and Schwarzschild spacetimes T is again a Killing parameter, and in de Sitter space it is cosmological proper time. For Bose-Einstein condensate analog black holes, T is the laboratory time [22].

Hence when the initial Cauchy surface contains components J that are horizons, since well-behaved particle states are defined with respect to λ_J , in the bulk of the spacetime those modes oscillate in $\lambda_J \sim e^{\pm \kappa_J T} e^{\pm \kappa_J R}$. It is this exponential relation between λ_J and $\kappa_J T$ that gives rise to a contribution of $\kappa_J T$ to G . Further, we see that the additivity $G = \sum_J \kappa_J T + \dots$ arises when the Cauchy surface contains several components.

One might be concerned that the collapsing null shell example, in which \mathcal{H}_b^- does not exist, does not fall into this description. However Hawking's original calculation [1] of black hole radiation from a horizon formed by gravitational collapse uses precisely this geometrical structure. Equation (2.16) in [1] relates the affine parameter of an outwardly propagating null geodesic infinitesimally close to \mathcal{H}_b^+ to good coordinates in the asymptotically flat past where the geodesic originates. Some relevant details of the steps involved are given in [35].

V. VELOCITY CORRELATION FUNCTION

In this section the two-point function for the field velocities $\partial_T \phi$ is computed. For comparison we first record the 2D Minkowski result. Using the freely falling particle states and coordinates defined in (4.1), (4.2) gives

$$2\pi \langle \partial_{t_1} \phi(x_1) \partial_{t_2} \phi(x_2) \rangle = -\frac{1}{(u_2 - u_1)^2} - \frac{1}{(v_2 - v_1)^2} . \quad (5.1)$$

So the correlation function is negative definite, goes to zero at null and spacelike infinity, and at equal times $t_1 = t_2$ reduces to $-2/R^2$ with $R = |x_2 - x_1|$.

Returning to SdS, consider $\phi = F(U) + G(V)$, where in this section we set $U \equiv U_b$ and $V \equiv V_c$ for ease in reading. Then

$$\partial_T \phi = -\kappa_b U F'(U) - \kappa_c V G'(V) . \quad (5.2)$$

Hence

$$\begin{aligned} 2\pi g(x_1, x_2) &\equiv 2\pi \langle \partial_{T_1} \phi(x_1) \partial_{T_2} \phi(x_2) \rangle \\ &= \lim_{\omega_0 \rightarrow 0} \left\{ \kappa_b^2 U_1 U_2 \frac{\partial}{\partial U_1} \frac{\partial}{\partial U_2} \int_{x_0}^{\infty} \frac{dx}{x} \cos x + \kappa_c^2 V_1 V_2 \frac{\partial}{\partial V_1} \frac{\partial}{\partial V_2} \int_{y_0}^{\infty} \frac{dy}{y} \cos y \right\} , \end{aligned} \quad (5.3)$$

where $x_0 = \omega_0(U_2 - U_1)$ and $y_0 = \omega_0(V_2 - V_1)$. The limit $\omega_0 \rightarrow 0$ can be taken because after taking the derivatives there is no infrared divergence. The result is

$$\begin{aligned} 2\pi g(x_1, x_2) &= -\kappa_b^2 \frac{U_1 U_2}{(U_2 - U_1)^2} - \kappa_c^2 \frac{V_1 V_2}{(V_2 - V_1)^2} \\ &\equiv 2\pi g_U(U_1, U_2) + 2\pi g_V(V_1, V_2) . \end{aligned} \quad (5.4)$$

Since the result is symmetric in x_1 and x_2 , we have not explicitly symmetrized. The result (5.4) can be derived in alternative ways, which are discussed in Appendix B.

Some general features of $g(x_1, x_2)$ can be read off of (5.4). At equal times, unlike the two point function of the fields, g is independent of time since U and V are each a product of a function of T times a function of r , given in (2.19) and (2.20). If x_1 and x_2 are both in the same region (black hole, static, or cosmo) then g is negative. Suppose one starts with x_1 and x_2 both in the static region so $g < 0$, as in Minkowski spacetime. Moving x_1 to \mathcal{H}_b^+

and x_2 to \mathcal{H}_c^+ means that $U_1 = V_2 = 0$ so the correlation function vanishes. If the points are moved further apart so that x_1 is inside the black hole and x_2 is in the cosmological region, then $U_1 U_2 > 0$, $V_1 V_2 > 0$, and the correlation function is positive. Hence going to longer length scales by crossing both horizons bounding the static diamond changes the sign of g , in contrast to Minkowski spacetime.

To examine these changes in more detail, it is useful to write g_U and g_V in terms of the Schwarzschild null coordinates u and v using (2.8) and (2.10). The result is

$$2\pi g_U(u_1, u_2) = -\frac{\kappa_b^2}{4 \sinh^2 \left[\frac{\kappa_b}{2}(u_1 - u_2) \right]}, \quad r_1, r_2 < r_b \text{ or } r_1, r_2 > r_b, \quad (5.5a)$$

$$= \frac{\kappa_b^2}{4 \cosh^2 \left[\frac{\kappa_b}{2}(u_1 - u_2) \right]}, \quad r_1 < r_b < r_2 \text{ or } r_2 < r_b < r_1, \quad (5.5b)$$

$$2\pi g_V(v_1, v_2) = -\frac{\kappa_c^2}{4 \sinh^2 \left[\frac{\kappa_c}{2}(v_1 - v_2) \right]}, \quad r_1, r_2 < r_c \text{ or } r_1, r_2 > r_c, \quad (5.5c)$$

$$= \frac{\kappa_c^2}{4 \cosh^2 \left[\frac{\kappa_c}{2}(v_1 - v_2) \right]}, \quad r_1 < r_c < r_2 \text{ or } r_2 < r_c < r_1. \quad (5.5d)$$

In the analysis that follows, we assume that $T_1 = T_2 = T$ and that H is held fixed. Then from (2.3) it is seen that the cosmological radius is given by

$$Hr_c = \frac{1}{2} \left(-Hr_b + \sqrt{4 - 3H^2 r_b^2} \right). \quad (5.6)$$

The black hole has a maximum size, corresponding to a minimal size of the cosmological horizon, when $r_b = r_c = 1/(\sqrt{3}H)$. In this extremal case $\kappa_b = \kappa_c = 0$ so there is no Hawking radiation and no Unruh state.

Since $u \rightarrow \infty$ on the black hole horizon, if one point is fixed there and the other is elsewhere, $g_U(x_1, x_2) = 0$. Similarly if one point is fixed on the cosmological horizon and the other is elsewhere then $g_V(x_1, x_2) = 0$. Further, $g_U < 0$ for separations where the two points are on the same side of the black hole horizon, and $g_V < 0$ when the points are on the same side of the cosmological horizon. For these separations the points can come together and thus $g(x_1, x_2)$ always approaches $-\infty$ in this limit. For separations in which the points are on opposite sides of the black hole horizon $g_U > 0$ and has a maximum at $u_1 = u_2$. When the points are on opposite sides of the cosmological horizon the same happens for g_V , except

the maximum is at $v_1 = v_2$.

The above properties for g_V are illustrated in Fig. 2 where plots are shown of $g(x_1, x_2)$ as a function of r_2 when $r_1 = r_b$ for various values of r_b and hence $g = g_V$. They are illustrated for g_U in Fig. 3 where plots are shown of $g(x_1, x_2)$ as a function of r_2 when $r_1 = r_c$, and hence $g = g_U$. A comparison between the plots shows that the peak when the points are on either side of the appropriate horizon is larger for g_U than for g_V , since $\kappa_b > \kappa_c$.

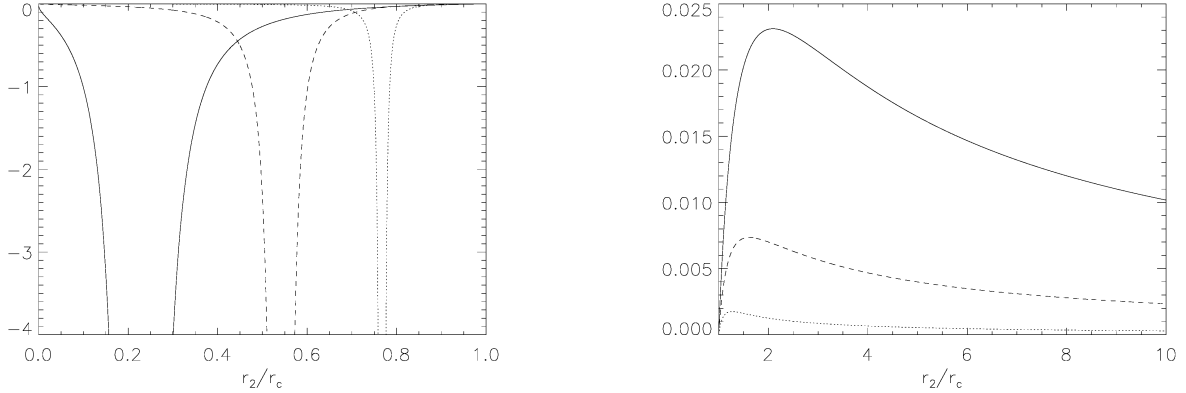


FIG. 2: The velocity correlation function is plotted as a function of $\frac{r_2}{r_c}$ with the point r_1 fixed on the black hole horizon r_b . The solid curves correspond to $H r_b = 0.2$, the dashed curves correspond to $H r_b = 0.4$, and the dotted curves correspond to $H r_b = 0.5$. The curves in the left panel are for $r_2 < r_c$ and those in the right panel are for $r_2 > r_c$, outside the cosmological horizon. The curves in the left panel diverge in the limit $r_2 \rightarrow r_1 = r_b$. Since the value of r_c depends on r_b when H is held fixed, this occurs at $\frac{r_b}{r_c} \approx 0.226, 0.542, 0.768$ for the solid, dashed, and dotted curves respectively.

We have seen that there is always a correlation peak in $g(x_1, x_2)$ if one point is fixed on a horizon and the other is separated from it. This will also occur when one point is fixed very close to a horizon. However, what happens when both points are on opposite sides of a horizon and neither point is close to the other horizon is more complicated. The reason is that there are often comparable contributions from g_U and g_V . In spite of this, if r_1 is fixed in the static region there is always a correlation peak at some r_2 in the cosmological region. To see this first note that for $r_b < r_2 < r_c$, $g(x_1, x_2) < 0$. As r_2 increases g_U remains negative but decreases. However, g_V goes through zero at $r_2 = r_c$ and is then positive for all larger values of r_2 . Now for $r_2 > r_c$, both g_U and g_V decrease in magnitude as r_2 increases.

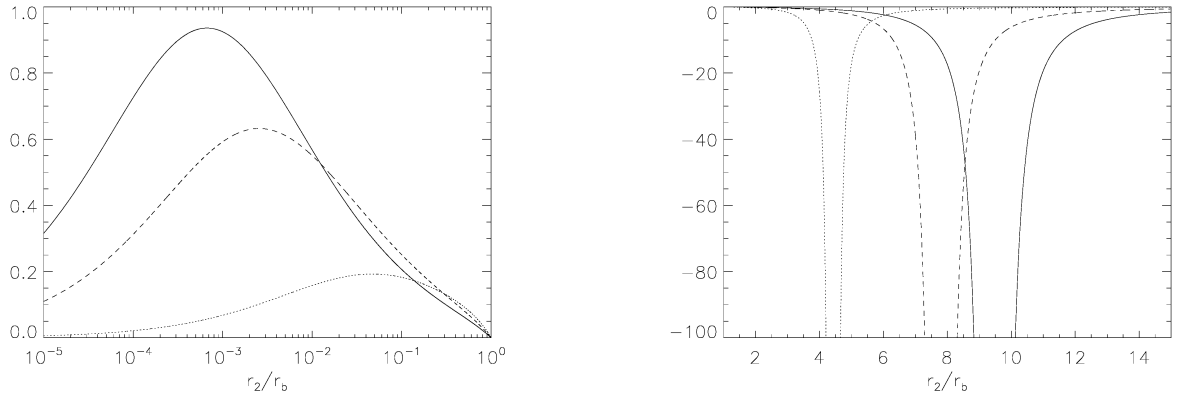


FIG. 3: The velocity correlation function is plotted as a function of $\frac{r_2}{r_b}$ with the point r_1 fixed on the cosmological horizon r_c . The solid curves correspond to $H r_b = 0.1$, the dashed curves correspond to $H r_b = 0.12$, and the dotted curves correspond to $H r_b = 0.2$. The curves in the left panel are for $r_2 < r_b$, inside the black hole, and those in the right panel are for $r_2 > r_b$. The curves in the right panel diverge in the limit $r_2 \rightarrow r_1 = r_c$. Since the value of r_c depends on r_b when H is held fixed, this occurs at $\frac{r_c}{r_b} \approx 9.46, 7.79, 4.42$ for the solid, dashed, and dotted curves respectively.

However, g_U which is negative decreases in magnitude faster than g_V because $\kappa_b > \kappa_c$. Thus eventually $g(x_1, x_2)$ changes sign, becoming positive. However, it also vanishes in the limit $r_2 \rightarrow \infty$. Therefore $g(x_1, x_2)$ has a maximum at some value of $r_2 > r_c$. This property is illustrated in Fig. 4. Note that as r_1 gets closer to the horizon, the peak gets smaller and is located at larger values of r_2 .

VI. FAR FIELD LIMIT AND RELATION TO THE BUNCH-DAVIES VACUUM

Calculations of the power spectrum due to quantum fluctuations in models of inflation start with the calculation of the two-point function for a scalar field in the Bunch-Davies vacuum. Ultimately we would like to know how this is changed by the presence of a black hole, or more accurately, by a population of black holes. It was established in Sec. IV C that in $2D$ the modes for the Unruh state in SdS coincide in the limit $M \rightarrow 0$ with the modes for the Bunch-Davies state. It is of interest to see how non-zero M modifies the modes for the Unruh state, and to see if there is any sense in which they approach those for the Bunch-Davies state in the cosmological region, far from the black hole.

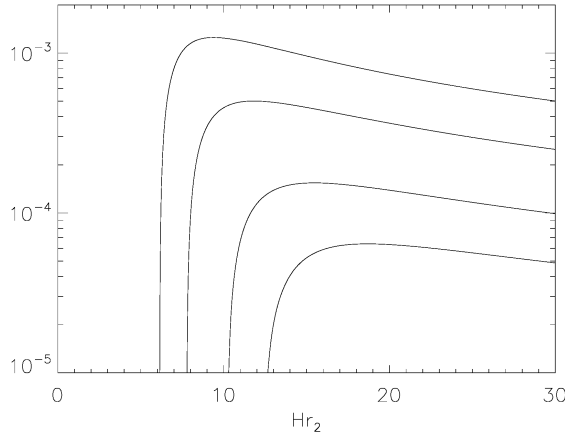


FIG. 4: The velocity correlation function is plotted as a function of Hr_2 for $Hr_b = 0.1$ and $Hr_c \approx 0.946$. The curves from top to bottom correspond to Hr_1 being fixed at $0.9Hrc$, $0.95Hrc$, $0.98Hrc$, and $0.99Hrc$ respectively. Since the purpose of this figure is to illustrate the changes in size and location of the peaks as the value of r_1 changes, only the parts of the curves with $r_2 > r_1$ and $g(r_1, r_2) > 0$ are shown.

A. Cosmological form of the metric

To make contact with an asymptotically FRW form of the metric, let

$$T = \tau + \xi(r) , \quad \text{where} \quad \frac{d\xi}{dr} = \frac{1}{f} \left(j + \frac{Hr}{(1 - \frac{2M}{r})^{1/2}} \right) . \quad (6.1)$$

This puts the metric into one of the “McVittie” forms analyzed in [36]

$$ds^2 = -fd\tau^2 - \frac{2Hr}{(1 - \frac{2M}{r})^{1/2}} drd\tau + \frac{dr^2}{1 - \frac{2M}{r}} . \quad (6.2)$$

Asymptotically, τ is the cosmological proper time coordinate. Next, transforming to an asymptotically comoving coordinate ρ such that

$$r = \left(1 + \frac{M}{2a\rho} \right)^2 a\rho , \quad a = e^{H\tau} . \quad (6.3)$$

yields the McVittie metric [37] in two dimensions.

$$ds^2 = a^2 \left[-\frac{\left(1 - \frac{M}{2a\rho}\right)^2}{\left(1 + \frac{M}{2a\rho}\right)^2} d\eta^2 + \left(1 + \frac{M}{2a\rho}\right)^4 d\rho^2 \right]. \quad (6.4)$$

In the last step we have changed to conformal time η defined by $d\eta = d\tau/a$ as before, $e^{H\tau} = -\frac{1}{H\eta}$, $-\infty < \eta < 0$.

To find the form of the Kruskal modes p_ω^b and p_ω^c , given in (3.1a), in the cosmological far field region, one needs the coordinate transformations when $r \gg r_c$, that is, when

$$a\rho = -\frac{\rho}{H\eta} \gg 1. \quad (6.5)$$

In this limit

$$\frac{M}{2a\rho} = -\frac{MH\eta}{2\rho} \ll 1, \quad (6.6)$$

corresponding to late times $\eta \rightarrow 0$ or large distances $\rho \rightarrow \infty$, where the metric (6.4) approaches the deSitter metric.

Equations (2.12) and (6.1) give $t = \tau - h(r) + \xi(r)$ with

$$\frac{d(\xi - h)}{dr} \simeq -\frac{1}{Hr} - \frac{M}{Hr^2}, \quad Hr \gg 1, \quad \frac{M}{r} \ll 1. \quad (6.7)$$

Integrating and changing to conformal time gives for a particular choice of integration constant

$$t \simeq -\frac{1}{H} \log(-H^2\eta r) + \frac{M}{Hr}. \quad (6.8)$$

For $r \gg r_c$, (2.17) becomes

$$2\kappa_c r_* \simeq \frac{2}{H} \frac{1+b}{r}, \quad b = \frac{H}{2} \left(r_c - \frac{2}{H} - \frac{\kappa_c r_b}{\kappa_b} + \frac{\kappa_c(r_c + r_b)}{\kappa_N} \right). \quad (6.9)$$

The definition of b is chosen so that $b = 0$ when $M = 0$. Combining the results gives

$$t \pm r_* \simeq -\frac{1}{H} \ln(-H^2\eta r) + \frac{1}{Hr} \left(M \pm \frac{1+b}{\kappa_c} \right). \quad (6.10)$$

Lastly, transforming from r to ρ in (6.10) gives the far field coordinate relations

$$\begin{aligned} V_c &\simeq \frac{H}{\kappa_c} (H\rho)^{\kappa_c/H-1} [\rho + (1 + M\kappa_c + b) \eta] , \\ U_b &\simeq \frac{H}{\kappa_b} (H\rho)^{\kappa_b/H-1} [-\rho + (1 - M\kappa_b + b) \eta] . \end{aligned} \quad (6.11)$$

One could scale ρ and η in such a way that V_c and U_b are proportional to $\rho \pm \eta$, but one cannot eliminate the overall factor of $\rho^{\kappa_c/H-1}$ in V_c or the factor of $\rho^{\kappa_b/H-1}$ in U_b . Therefore there is a significant difference between the behaviors of the modes for the Unruh state when $M > 0$ and the modes for the Bunch-Davies state when $M = 0$ even far from the black hole.

The mode $\exp(-i\omega U_b)$ is outgoing and it describes the black hole radiation arising from \mathcal{H}_b^- . In four dimensions there would be additional outgoing modes that start on \mathcal{H}_c^- inside the static patch, scatter off the spacetime geometry, and propagate out through \mathcal{H}_c^+ . These are longer wavelength modes that “pass over” the black hole without being absorbed. However, in $2D$ any mode that starts on the portion of \mathcal{H}_c^- in the static patch propagates directly into the black hole and does not reach the far field region – in this sense, all $2D$ black holes are the same size.

An indication of the effect of the black hole on the power spectrum is given by the difference in the Kruskal coordinates (6.11) from the $M = 0$ cosmological expressions $\eta \pm \rho$. With a black hole present $\kappa_c < H$, and we expect that this difference in the exponent of ρ will show up as a correction to the scale invariance of the power spectrum. However, since the differences between the mode solutions in $2D$ and $4D$ are qualitatively significant, we will end the $2D$ cosmological analysis here, and pursue the $4D$ SdS case in subsequent work. Nonetheless, we can get some guidance about the $4D$ case by looking at de Sitter space with no black hole, which we treat briefly next.

B. Two point function in de Sitter space in four dimensions

What features of the Green’s function does one expect to persist to $4D$? The intriguing result (3.10) that the time dependence of G is like $(\kappa_b + \kappa_c)T$ derives from (1) the exponential relation between the Kruskal coordinates and the (T, r) ones, (2) that the Cauchy surface is the union of \mathcal{H}_b^- and \mathcal{H}_c^- , (3) that there is no scattering in $2D$, and (4) that there is an infrared divergence leading to the lower limit cutoff ω_0 in (3.6). The sequence of $2D$

examples in Section (IV) illustrate how these properties contribute to the resulting time dependence. Probably the most relevant difference from two to four dimensions is that in $4D$ there is scattering, so even spherically symmetric waves do not propagate as pure ingoing or outgoing modes. This leads to technical complications in extracting the time dependence of G . However, when there is no black hole the modes in $4D$ de Sitter do propagate in a simple way. So let us look at the well studied two-point function in the Bunch-Davies vacuum of de Sitter space.

In four dimensions

$$\phi = \frac{1}{(2\pi)^{3/2}} \int d^3k \left[b_{\vec{k}} u_k(\eta) e^{i\vec{k}\cdot\vec{x}} + b_{\vec{k}}^\dagger u_k^*(\eta) e^{-i\vec{k}\cdot\vec{x}} \right], \quad (6.12)$$

with

$$u_k(\eta) = -\frac{H\eta}{\sqrt{2k}} \left(1 - \frac{i}{k\eta} \right) e^{-ik\eta}, \quad (6.13)$$

where \vec{k} is the co-moving wave vector and x^j are comoving spatial coordinates. Following the same steps as before and setting $\eta' = \eta$ gives

$$\langle 0 | \{\phi(x), \phi(x')\} | 0 \rangle = \frac{H^2}{2\pi^2} \int_{k_0}^{\infty} dk \frac{\sin kx}{k^2 x} (1 + k^2 \eta^2), \quad (6.14)$$

where k_0 is a long wavelength cut-off and $x = |\vec{x} - \vec{x}'|$ is the comoving spatial distance between the two points. Rather than getting the result at the end of inflation, we are interested in the time dependence of the correlation function during inflation, for points at the same cosmological time and separated by a proper spatial distance R . Setting $x = R/a = -H\eta R$, and $q = -k\eta$ the integral (6.12) becomes

$$\langle 0 | \phi(x) \phi(x') | 0 \rangle = \frac{H^2}{4\pi^2} \int_{q_0}^{\infty} \frac{dq}{q} \frac{\sin HqR}{HqR} (1 + q^2), \quad q_0 = \frac{k_0}{H} e^{-H\tau}. \quad (6.15)$$

At fixed proper distance R the time dependence of the correlation function is carried by the lower limit of integration q_0 . Taking the τ derivative and expanding about $q_0 = 0$ gives

$$\frac{\partial}{\partial \tau} \langle 0 | \{\phi(x), \phi(x')\} | 0 \rangle = \frac{H^3}{2\pi^2} \frac{\sin Hq_0 R}{Hq_0 R} (1 + q_0^2) \quad (6.16a)$$

$$\simeq \frac{H^3}{2\pi^2} \left(1 + \frac{k_0^2}{H^2} (1 - \frac{1}{6} H^2 R^2) e^{-2H\tau} \right). \quad (6.16b)$$

The rate is proportional to H^3 rather than H as in $2D$, but the “extra” factor of H^2 is simply due to the fact that in $2D$ the scalar field is dimensionless but in $4D$ has dimensions length^{-1} , and H is the only dimensionful quantity available. The corresponding linear growth in terms of the proper time τ of the correlation function has been previously obtained in [38] and a linear growth in proper time for $\langle \phi^2 \rangle$ has been found in [38, 39]. Hence the leading long wavelength or late time term qualitatively agrees with the $2D$ result. This suggests that an interesting topic for future study is whether the time dependence of $2D$ SdS persists in $4D$ SdS, in the late time limit.

VII. CONCLUDING REMARKS

Two-dimensional SdS is a convenient spacetime to study the effects of horizons on quantum fields since the spacetime contains two horizons, and the wave equation can be solved exactly. This means that the effects of scattering are not present and so the effects of the causal structure on the initial waveforms are highlighted.

The symmetric two-point function was computed analytically in the generalized Unruh vacuum using an infrared cutoff ω_0 , that is assumed to be fixed in size but can be made to be arbitrarily small. Its behavior was analyzed on surfaces of constant T , where T is a timelike and well-behaved coordinate throughout the spacetime. It was found that the time rate of change of the two-point function is

$$\frac{d}{dT}G(T, r_1; T, r_2) = \kappa_b + \kappa_c . \quad (7.1)$$

To determine how general this result is the two-point function was computed in several $2D$ spacetimes that contain past horizons. In each case it was found that

$$\frac{d}{dT}G(T, r_1; T, r_2) = \sum_J \kappa_J , \quad (7.2)$$

where the sum is over any past horizons used to define the vacuum on an early time Cauchy surface. In cases where both a past horizon and past null infinity exists, the sum can be thought of as including a contribution from the latter surface since it has a surface gravity of zero. The result for G is actually more general than that, also holding at late times for a

Schwarzschild black hole that forms from collapse of a null shell. This is an example of the fact that a quantum field in eternal Schwarzschild spacetime in the Unruh state has the same late time behavior as a quantum field in the *in* vacuum state in a spacetime where a black hole forms from collapse. This constant rate of growth of $G(x, x')$ appears to depend on both the existence of a horizon and the existence of an infrared divergence in this two-point function.

The two point function of the field velocities ($\partial_T \phi$) was also computed. It has no infrared divergence and is time-independent. However, it exhibits some interesting spatial structure. In the static region its behavior is similar to that of the velocity two-point function in Minkowski spacetime, but it changes sign as the points move further apart crossing the horizons. In addition, peaks in the correlation function develop. The height and placement of the peaks depend on the size of the black hole as well as the location of each point.

It is unknown whether the linear growth in T of G generalizes to 4D for SdS, but there are two hints that it may do so. First this growth occurs at late times in 4D de Sitter. Second, there is an infrared divergence in G in 4D SdS [40]. We plan to address this question in a future publication. We do expect that similar structure to that found in the velocity correlation function will occur in the 4D case for both Schwarzschild spacetime, SdS, and de Sitter space. In fact there is likely to be a richer structure in the 4D case because the mode functions undergo scattering effects. This has been seen in the case of 2D BEC analog spacetimes when an effective potential in the phonon mode equation is included [22] and thus scattering effects occur. While one may be less interested in these effects for Schwarzschild spacetime where one point of the two-point function must be inside the event horizon, they occur in a potentially measurable way for SdS when one point is inside the cosmological horizon but outside the black hole horizon and the other is outside the cosmological horizon.

Investigating quantum effects in 2D SdS is a good place to begin studying the effects of primordial black holes in cosmology. Nonetheless, one really wants the calculation in four dimensions, extending the results of [13]. Eventually one would like to know, for what size black hole is there an observable signature in the CMBR? Or, more realistically, what distributions of primordial black holes give a signal in the CMBR, and is it distinguishable from other sources of non-scale invariance.

Acknowledgments

We thank David Kastor and Alessandro Fabbri for useful conversations. This work was supported in part by the National Science Foundation under Grants No. PHY-1505875 and PHY-1912584 to Wake Forest University. Some of the plots were made using the WFU DEAC cluster; we thank the WFU Provost’s Office and Information Systems Department for their generous support.

Appendix A: Alternative computation of the two-point function

For a BEC analog black hole in two dimensions and for any static spherically symmetric black hole in four dimensions the wave equation is not separable in Kruskal coordinates, which makes it difficult to find analytic solutions with the appropriate initial data for the Unruh state on the past horizon(s). To make the calculations tractable one can expand the Kruskal modes in terms of a complete set of mode functions that are positive frequency with respect to the static Schwarzschild time coordinate t . The mode equation is separable in the static coordinates for the BEC system and for a static spherically symmetric black hole in $4D$. Then one can use the result to construct the two-point function and any other function obtained from it in terms of the modes that are positive frequency with respect to t .

Substituting into the expression for the two-point function in terms of the Kruskal modes one obtains a triple integral over products of the mode functions and their expansion coefficients. One of these integrals is only over the expansion coefficients, and this is computed last. If it is computed first then one gets a Dirac delta function, which leaves only one integral that is nontrivial to compute.

Following this procedure for a 2D BEC analog black hole when the effective potential in the mode equation is ignored yields an expression for the two-point function that only depends on the time independent differences $u_2 - u_1$ and $v_2 - v_1$ [22].² Thus there is no linear growth in T when $T_2 = T_1 = T$. It is straight-forward to show that exactly the same thing happens for Schwarzschild spacetime in 2D and for SdS in 2D. Hence the two methods give different answers.

To find where the error is, we give an example of the alternative calculation for one

² If the effective potential is included the two-point function depends on the time difference $t_2 - t_1$.

contribution to the two-point function in SdS in the static patch between the black hole and cosmological horizons. The generalization to the other contributions to the two-point function, to other regions of SdS, or to other spacetimes in which the Unruh state can be defined should be clear.

We start with the two point function in (3.6). Instead of integrating directly over the mode functions one can expand them in terms of the modes that are positive frequency with respect to the time t in the static region of SdS. In 2D SdS a complete set of modes in the static patch that is positive frequency with respect to t is

$$\begin{aligned} p_{\omega}^{\mathcal{H}_c^-}(v) &= \frac{e^{-i\omega v}}{\sqrt{4\pi\omega}}, \\ p_{\omega}^{\mathcal{H}_b^-}(u) &= \frac{e^{-i\omega u}}{\sqrt{4\pi\omega}}. \end{aligned} \quad (\text{A1})$$

The Kruskal modes can be expanded in terms of these,

$$p_w^b = \int_0^\infty d\omega_1 \left[\alpha_{\omega\omega_1}^b p_{\omega_1}^{\mathcal{H}_b^-} + \beta_{\omega\omega_1}^b p_{\omega_1}^{\mathcal{H}_b^- *} \right], \quad (\text{A2a})$$

$$p_w^c = \int_0^\infty d\omega_1 \left[\alpha_{\omega\omega_1}^c p_{\omega_1}^{\mathcal{H}_c^-} + \beta_{\omega\omega_1}^c p_{\omega_1}^{\mathcal{H}_c^- *} \right]. \quad (\text{A2b})$$

The Bogolubov coefficients can be found using the fact that the modes in (A1) are orthonormal with respect to the usual scalar product which is [41]

$$(p_1, p_2) = -i \int_{\Sigma} d\Sigma n^\mu [p_1(x) \overset{\leftrightarrow}{\partial}_\mu p_2^*(x)], \quad (\text{A3})$$

with n^μ a future-directed unit vector orthogonal to the hypersurface Σ which is a Cauchy surface. The Cauchy surface we use is the union between the two past horizons \mathcal{H}_b^- and \mathcal{H}_c^- . The modes $p_{\omega_1}^{\mathcal{H}_b^-}$ are zero on \mathcal{H}_c^- and the modes $p_{\omega_1}^{\mathcal{H}_c^-}$ are zero on \mathcal{H}_b^- . The result for $\alpha_{\omega\omega_1}^b$ is

$$\alpha_{\omega\omega_1}^b = (p_w^b, p_{\omega_1}^{\mathcal{H}_b^-}) = -\frac{i}{4\pi\sqrt{\omega\omega_1}} \int_{-\infty}^0 dU_b e^{-i\omega U_b} \frac{\overset{\leftrightarrow}{\partial}}{\partial U_b} e^{i\omega_1 u}. \quad (\text{A4})$$

For the integral to be well defined one can insert into the integrand $(-\kappa_b U_b)^\delta e^{\epsilon\kappa_b U_b}$, where the integrating factors $\delta > 0$ and $\epsilon > 0$ are to be set equal to zero once all calculations using $\alpha_{\omega\omega_1}^b$ are finished. Then, integrating by parts so that for both terms the derivative acts on

the mode function to the right gives

$$\alpha_{\omega\omega_1}^b = -\frac{i}{2\pi\sqrt{\omega\omega_1}} \int_{-\infty}^0 dU_b e^{-i\omega U_b + \epsilon\kappa_b U_b} \frac{i\omega_1 - \kappa_b \delta}{(-\kappa_b U_b)^{i\frac{\omega_1}{\kappa_b} + 1 - \delta}}. \quad (\text{A5})$$

It turns out that the factor of δ in the numerator can be set equal to zero immediately. Doing that and changing the integration variable to $Z = -\kappa_b U_b$ gives [42]

$$\begin{aligned} \alpha_{\omega\omega_1}^b &= \frac{1}{2\pi\kappa_b} \sqrt{\frac{\omega_1}{\omega}} \int_0^\infty dZ Z^{-i\frac{\omega_1}{\kappa_b} - 1 + \delta} e^{i\frac{\omega}{\kappa_b} Z - \epsilon Z} \\ &= \frac{1}{2\pi\kappa_b} \sqrt{\frac{\omega_1}{\omega}} \left(-i\frac{\omega}{\kappa_b} + \epsilon \right)^{\frac{i\omega_1}{\kappa_b}} \Gamma \left(\delta - i\frac{\omega_1}{\kappa_b} \right). \end{aligned} \quad (\text{A6})$$

The other Bogolubov coefficients are computed in a similar way with the result:

$$\beta_{\omega\omega_1}^b = -(p_\omega^b, p_{\omega_1}^{\mathcal{H}_b^- *}) = \frac{1}{2\pi\kappa_b} \sqrt{\frac{\omega_1}{\omega}} \left(-i\frac{\omega}{\kappa_b} + \epsilon \right)^{\frac{-i\omega_1}{\kappa_b}} \Gamma \left(\delta + i\frac{\omega_1}{\kappa_b} \right) \quad (\text{A7a})$$

$$\alpha_{\omega\omega_1}^c = (p_\omega^c, p_{\omega_1}^{\mathcal{H}_c^-}) = \frac{1}{2\pi\kappa_c} \sqrt{\frac{\omega_1}{\omega}} \left(-i\frac{\omega}{\kappa_c} + \epsilon \right)^{\frac{i\omega_1}{\kappa_c}} \Gamma \left(\delta - i\frac{\omega_1}{\kappa_c} \right) \quad (\text{A7b})$$

$$\beta_{\omega\omega_1}^c = -(p_\omega^c, p_{\omega_1}^{\mathcal{H}_c^- *}) = \frac{1}{2\pi\kappa_c} \sqrt{\frac{\omega_1}{\omega}} \left(-i\frac{\omega}{\kappa_c} + \epsilon \right)^{\frac{-i\omega_1}{\kappa_c}} \Gamma \left(\delta + i\frac{\omega_1}{\kappa_c} \right). \quad (\text{A7c})$$

Substituting (A7) into (A2) and then substituting the result into (3.6) gives a number of terms each with a triple integral. For illustration purposes we shall just take one term which comes the product $p_\omega^b(x)p_\omega^b(x')$, the first term in the integrand in (3.6). This example term is

$$\begin{aligned} [G(x, x')]_{ex} &= \int_0^\infty d\omega \int_0^\infty d\omega_1 \int_0^\infty d\omega_2 \alpha_{\omega\omega_1}^b \alpha_{\omega\omega_2}^{b*} p_{\omega_1}^b p_{\omega_2}^{b*} \\ &= \frac{1}{16\pi^3 \kappa_b^2} \int_0^\infty \frac{d\omega}{\omega} \int_0^\infty d\omega_1 \int_0^\infty d\omega_2 \left(-i\frac{\omega}{\kappa_b} + \epsilon \right)^{\frac{i\omega_1}{\kappa_b}} \left(i\frac{\omega}{\kappa_b} + \epsilon \right)^{\frac{-i\omega_2}{\kappa_b}} \\ &\quad \times \Gamma \left(\delta - i\frac{\omega_1}{\kappa_b} \right) \Gamma \left(\delta + i\frac{\omega_2}{\kappa_b} \right) e^{-i\omega_1 u + i\omega_2 u'} \end{aligned} \quad (\text{A8})$$

Interchanging the order of integration gives

$$\begin{aligned} [G(x, x')]_{ex} &= \frac{1}{16\pi^3\kappa_b^2} \int_0^\infty d\omega_1 \int_0^\infty d\omega_2 \Gamma\left(\delta - i\frac{\omega_1}{\kappa_b}\right) \Gamma\left(\delta + i\frac{\omega_2}{\kappa_b}\right) e^{-i\omega_1 u + i\omega_2 u'} e^{\frac{\pi(\omega_1 + \omega_2)}{2\kappa_b}} \\ &\quad \times \int_0^\infty \frac{d\omega}{\omega} \left(\frac{\omega}{\kappa_b}\right)^{\frac{i(\omega_1 - \omega_2)}{\kappa_b}}, \end{aligned} \quad (\text{A9})$$

where ϵ has been set equal to zero. The last integral can be computed by making the change of variable $\kappa z = \log \kappa_b^{-1}\omega$ with the result that it is equal to $2\pi\delta(\omega_1 - \omega_2)$. Then integrating over ω_2 gives

$$[G(x, x')]_{ex} = \frac{1}{8\pi^2\kappa_b} \int_0^\infty d\omega_1 \left| \Gamma\left(\delta - i\frac{\omega_1}{\kappa_b}\right) \right|^2 e^{\frac{\pi\omega_1}{\kappa_b}} e^{-i\omega_1(u - u')}. \quad (\text{A10})$$

This integral is infrared divergent when $\delta = 0$, so an infrared cutoff λ must be inserted, giving

$$[G(x, x')]_{ex} = \frac{1}{8\pi} \int_\lambda^\infty d\omega_1 \frac{e^{\frac{\pi\omega_1}{\kappa_b}}}{\omega_1 \sinh\left(\frac{\pi\omega_1}{\kappa_b}\right)} e^{-i\omega_1(u - u')}. \quad (\text{A11})$$

In either form it is clear that $[G(x, x')]_{ex}$ is a function of $u - u'$, so for $T' = T$ there is no T dependence in $[G(x, x')]_{ex}$. This result holds for all nonvanishing terms in $G(x, x')$. Thus when the order of integration is switched, the linear growth in T of $G(x, x')$ disappears.

Therefore this second method of computing $G(x, x')$ misses the time dependent piece. Both methods require an infrared cutoff, but the two calculations insert the cutoff in different ways. If one integrates directly over the Kruskal modes, as done in Section (III), then the cutoff is inserted in the single mode integral over the frequencies. If one expands in the static basis, then in getting the delta functions one integrates over all values of the frequencies of the Kruskal modes. The infrared cutoff is then inserted on the remaining integral after the delta functions have been integrated over. We view the first method as defining the two-point function. The use of the second method for BEC analog black holes has lead to the time growth being missed. We have also not found it mentioned for either static black holes or black holes that form from collapse in 2D.

Finally, it is worth pointing out that if one computes a quantity such as the velocity correlation function, then the infrared divergence in the integral over ω is eliminated and it is possible to interchange the order of integration. As pointed out in Sec. V, the velocity

correlation function has no dependence on T as would be expected.

Appendix B: Alternative computation of the velocity correlation function

The derivation of (5.4) involves computing the derivatives first and then setting the infrared cutoff ω_0 to zero. The same procedure can also be used to derive (5.4) from (3.9) or equivalently from (3.7). In these two latter cases one computes the integral first and then computes the derivatives.

There is an alternative way of deriving (5.4) that eliminates the necessity for an infrared cutoff. One can start with $\langle \partial_{T_1}\phi \partial_{T_2}\phi \rangle$, use the mode expansion (3.2) and compute the derivatives before computing the integral. In this case one has

$$\begin{aligned} 2\pi g(x, x') &= \kappa_b^2 U_1 U_2 \int_0^\infty d\omega \frac{\partial}{\partial U_1} \frac{\partial}{\partial U_2} \frac{\cos(\omega \Delta U)}{\omega} + \kappa_c^2 V_1 V_2 \int_0^\infty d\omega \frac{\partial}{\partial V_1} \frac{\partial}{\partial V_2} \frac{\cos(\omega \Delta V)}{\omega} , \\ &= \kappa_b^2 U_1 U_2 \int_0^\infty d\omega \omega \cos(\omega \Delta U) + \kappa_c^2 V_1 V_2 \int_0^\infty d\omega \omega \cos(\omega \Delta V) , \end{aligned} \quad (\text{B1})$$

where $U = U_b$, $V = V_c$, $\Delta U = U_1 - U_2$ and $\Delta V = V_1 - V_2$. Note that we have been able to set $\omega_0 = 0$ because there is no longer an infrared divergence in the integrand. Since the two integrals have exactly the same form we'll focus on the first one which is

$$I = \int_0^\infty d\omega \omega \cos \omega \Delta U , \quad (\text{B2})$$

with $\Delta U = U_1 - U_2$. The integrand oscillates with an amplitude that is unbounded in the limit $\omega \rightarrow \infty$. However, because of the oscillatory factor it can be evaluated in terms of distributions. Inserting the Heavyside function $H(\omega)$ the range of integration can be extended over the real line and the integral becomes a Fourier transform. With the aid of Table 1 in reference [43] one has

$$\begin{aligned} I &= \mathcal{R}e \int_{-\infty}^\infty d\omega \omega H(\omega) e^{-i\omega \Delta U} \\ &= \mathcal{R}e \left(2\pi i \delta^{(1)}(\Delta U) - \frac{1}{(\Delta U)^2} \right) \\ &= -\frac{1}{(\Delta U)^2} \end{aligned} \quad (\text{B3})$$

where $\delta^{(1)}(x)$ is the first derivative of the delta function. Hence either order of integration and differentiation gives the same result.

- [1] S. W. Hawking, “Particle Creation by Black Holes,” *Commun. Math. Phys.* **43**, 199 (1975) Erratum: [Commun. Math. Phys. **46**, 206 (1976)].
- [2] G. W. Gibbons and S. W. Hawking, “Cosmological Event Horizons, Thermodynamics, and Particle Creation,” *Phys. Rev. D* **15**, 2738 (1977). doi:10.1103/PhysRevD.15.2738
- [3] A. H. Guth and S. Y. Pi, “Fluctuations in the New Inflationary Universe,” *Phys. Rev. Lett.* **49**, 1110-1113 (1982) doi:10.1103/PhysRevLett.49.1110
- [4] A. A. Starobinsky, “Dynamics of Phase Transition in the New Inflationary Universe Scenario and Generation of Perturbations,” *Phys. Lett. B* **117**, 175-178 (1982) doi:10.1016/0370-2693(82)90541-X
- [5] Y. B. Zel'dovich and I. D. Novikov, 1966, “The Hypothesis of Cores Retarded during Expansion and the Hot Cosmological Model,” *Astronomicheskii Zhurnal*, Vol. 43, 758.
- [6] B. J. Carr and S. W. Hawking, “Black holes in the early Universe,” *Mon. Not. Roy. Astron. Soc.* **168**, 399-415 (1974)
- [7] J. García-Bellido, “Massive Primordial Black Holes as Dark Matter and their detection with Gravitational Waves,” *J. Phys. Conf. Ser.* **840**, no.1, 012032 (2017) doi:10.1088/1742-6596/840/1/012032 [arXiv:1702.08275 [astro-ph.CO]].
- [8] S. Bird, I. Cholis, J. B. Muñoz, Y. Ali-Haïmoud, M. Kamionkowski, E. D. Kovetz, A. Racanelli and A. G. Riess, “Did LIGO detect dark matter?”, *Phys. Rev. Lett.* **116**, no.20, 201301 (2016) doi:10.1103/PhysRevLett.116.201301 [arXiv:1603.00464 [astro-ph.CO]].
- [9] E. Bianchi, A. Gupta, H. M. Haggard and B. S. Sathyaprakash, “Small Spins of Primordial Black Holes from Random Geometries: Bekenstein-Hawking Entropy and Gravitational Wave Observations,” [arXiv:1812.05127 [gr-qc]].
- [10] N. Padilla, J. Magana, J. Sureda and I. Araya, “Power spectrum of density fluctuations, halo abundances and clustering with primordial black holes,” [arXiv:2010.06470 [astro-ph.CO]].
- [11] V. F. Mukhanov, H. A. Feldman and R. H. Brandenberger, “Theory of cosmological perturbations. Part 1. Classical perturbations. Part 2. Quantum theory of perturbations. Part 3. Extensions,” *Phys. Rept.* **215**, 203-333 (1992) doi:10.1016/0370-1573(92)90044-Z

[12] J. Chluba, J. Hamann and S. P. Patil, “Features and New Physical Scales in Primordial Observables: Theory and Observation,” *Int. J. Mod. Phys. D* **24**, no.10, 1530023 (2015) doi:10.1142/S0218271815300232 [arXiv:1505.01834 [astro-ph.CO]].

[13] T. Prokopec and P. Reska, “Scalar cosmological perturbations from inflationary black holes,” *JCAP* **1103**, 050 (2011) doi:10.1088/1475-7516/2011/03/050 [arXiv:1007.3851 [gr-qc]].

[14] H. T. Cho, K. W. Ng and I. C. Wang, “Inflaton fluctuations in the presence of cosmological defects,” *JCAP* **11**, 023 (2014) doi:10.1088/1475-7516/2014/11/023 [arXiv:1405.5804 [hep-th]].

[15] H. Firouzjahi, A. Karami and T. Rostami, “Primordial inhomogeneities from massive defects during inflation,” *JCAP* **10**, 023 (2016) doi:10.1088/1475-7516/2016/10/023 [arXiv:1605.08338 [astro-ph.CO]].

[16] W. G. Unruh, “Notes on black hole evaporation,” *Phys. Rev. D* **14**, 870 (1976) doi:10.1103/PhysRevD.14.870

[17] D. Markovic and W. G. Unruh, “Vacuum for a massless scalar field outside a collapsing body in de Sitter space-time,” *Phys. Rev. D* **43**, 332 (1991). doi:10.1103/PhysRevD.43.332

[18] R. Gregory, D. Kastor and J. Traschen, “Black Hole Thermodynamics with Dynamical Lambda,” *JHEP* **1710**, 118 (2017) doi:10.1007/JHEP10(2017)11 [arXiv:1707.06586 [hep-th]].

[19] R. Gregory, D. Kastor and J. Traschen, “Evolving Black Holes in Inflation,” *Class. Quant. Grav.* **35**, no. 15, 155008 (2018) doi:10.1088/1361-6382/aacec2 [arXiv:1804.03462 [hep-th]].

[20] R. Balbinot, A. Fabbri, S. Fagnocchi, A. Recati and I. Carusotto, “Non-local density correlations as signal of Hawking radiation in BEC acoustic black holes,” *Phys. Rev. A* **78**, 021603 (2008) doi:10.1103/PhysRevA.78.021603 [arXiv:0711.4520 [cond-mat.other]].

[21] I. Carusotto, S. Fagnocchi, A. Recati, R. Balbinot and A. Fabbri, “Numerical observation of Hawking radiation from acoustic black holes in atomic BECs,” *New J. Phys.* **10**, 103001 (2008) doi:10.1088/1367-2630/10/10/103001 [arXiv:0803.0507 [cond-mat.other]].

[22] P. R. Anderson, R. Balbinot, A. Fabbri and R. Parentani, “Hawking radiation correlations in Bose Einstein condensates using quantum field theory in curved space,” *Phys. Rev. D* **87**, no.12, 124018 (2013) doi:10.1103/PhysRevD.87.124018. [arXiv:1301.2081 [gr-qc]].

[23] J. Steinhauer, “Observation of quantum Hawking radiation and its entanglement in an analogue black hole,” *Nature Phys.* **12**, 959 (2016) doi:10.1038/nphys3863 [arXiv:1510.00621 [gr-qc]].

[24] J. R. Muñoz de Nova, K. Golubkov, V. I. Kolobov and J. Steinhauer, “Observation of thermal Hawking radiation and its temperature in an analogue black hole,” *Nature* **569**, no.7758, 688-691 (2019) doi:10.1038/s41586-019-1241-0 [arXiv:1809.00913 [gr-qc]].

[25] P. O. Fedichev and U. R. Fischer, “Gibbons-Hawking effect in the sonic de Sitter space-time of an expanding Bose-Einstein-condensed gas,” *Phys. Rev. Lett.* **91**, 240407 (2003) doi:10.1103/PhysRevLett.91.240407 [arXiv:cond-mat/0304342 [cond-mat]].

[26] Y. Qiu and J. Traschen, “Black Hole and Cosmological Particle Production in Schwarzschild de Sitter,” *Class. Quant. Grav.* **37**, no.13, 135012 (2020) doi:10.1088/1361-6382/ab8bba [arXiv:1908.02737 [hep-th]].

[27] L. Aalsma, M. Parikh and J. P. Van Der Schaar, “Back(reaction) to the Future in the Unruh-de Sitter State,” *JHEP* **11**, 136 (2019) doi:10.1007/JHEP11(2019)136 [arXiv:1905.02714 [hep-th]].

[28] S. Massar and R. Parentani, “From vacuum fluctuations to radiation. 2. Black holes,” *Phys. Rev. D* **54**, 7444-7458 (1996) doi:10.1103/PhysRevD.54.7444

[29] A. Fabbri and J. Navarro-Salas, *Modeling black hole evaporation* (Imperial College Press, London, UK, 2005).

[30] M. R. R. Good, P. R. Anderson and C. R. Evans, “Mirror Reflections of a Black Hole,” *Phys. Rev. D* **94**, no.6, 065010 (2016) doi:10.1103/PhysRevD.94.065010 [arXiv:1605.06635 [gr-qc]].

[31] F. Michel, J. F. Coupéchoux and R. Parentani, “Phonon spectrum and correlations in a transonic flow of an atomic Bose gas,” *Phys. Rev. D* **94**, no.8, 084027 (2016) doi:10.1103/PhysRevD.94.084027 [arXiv:1605.09752 [cond-mat.quant-gas]].

[32] R. A. Dudley, A. Fabbri, P. R. Anderson and R. Balbinot, “Correlations between a Hawking particle and its partner in a 1+1D Bose-Einstein condensate analog black hole,” *Phys. Rev. D* **102**, no.10, 105005 (2020) doi:10.1103/PhysRevD.102.105005 [arXiv:2008.01433 [gr-qc]].

[33] R. M. Wald, *General Relativity*, University of Chicago Press (1984), chpt. 12.

[34] B. Carter, ”Mathematical Foundations of the Theory of Relativistic Stellar and Black Hole Configurations”, in *Gravitation in Astrophysics Cargese 1986*, ed. B. Carter and J. Hartle, Plenum Press (1986).

[35] J. H. Traschen, “An Introduction to black hole evaporation,” [arXiv:gr-qc/0010055 [gr-qc]].

[36] N. Kaloper, M. Kleban and D. Martin, “McVittie’s Legacy: Black Holes in an Expanding Universe,” *Phys. Rev. D* **81**, 104044 (2010) doi:10.1103/PhysRevD.81.104044 [arXiv:1003.4777

[hep-th]].

- [37] G. C. McVittie, “The mass-particle in an expanding universe,” *Mon. Not. Roy. Astron. Soc.* **93**, 325 (1933). doi:10.1093/mnras/93.5.325
- [38] B. Allen, “Vacuum States in de Sitter Space,” *Phys. Rev. D* **32**, 3136 (1985).
- [39] A. Vilenkin and L. H. Ford, ‘Gravitational Effects upon Cosmological Phase Transitions,’ *Phys. Rev. D* **26**, 1231 (1982).
- [40] P. R. Anderson, A. Fabbri, and R. Balbinot, “Low frequency gray-body factors and infrared divergences: rigorous results,” *Phys. Rev. D* **91**, 064061 (2015).
- [41] N. D. Birrell and P. C. W. Davies, “Quantum fields in Curved Space”, Cambridge University Press (Cambridge, England) (1982).
- [42] See for example, I. S. Gradshteyn and I. M. Ryzhik, “Table of Integrals, Series, and Products: Corrected and Enlarged Edition”, (Academic Press, Inc., London) (1980).
- [43] M. J. Lighthill, “Introduction to Fourier Analysis and Generalised Functions,” Cambridge University Press (1975).